Journal of Materials Chemistry A

RSC Publishing

PAPER

View Article Online
View Journal | View Issue

Cite this: J. Mater. Chem. A, 2013, 1, 4525

A photoluminescent microporous metal organic anionic framework for nitroaromatic explosive sensing†

Yun-Shan Xue,[a] Yabing He,[b] Lian Zhou,[a] Fei-Jian Chen,[a] Yan Xu,[c] Hong-Bin Du,*[a] Xiao-Zeng You[a] and Banglin Chen[b]

Received 16th November 2012
Accepted 30th January 2013

DOI: 10.1039/c3ta01118f

www.rsc.org/MaterialsA

By using the octadentate ligand tetrakis[(3,5-dicarboxyphenoxy)methyl] methane (H_8L), a rare (4,8)-*scu* type microporous coordination polymer, $[In_2L][NH_2(CH_3)_2]_2\cdot(DMF)_4(H_2O)_{16}$, was synthesized and structurally characterized. The compound possesses an anionic three-dimensional open framework and exhibits permanent porosity with selective gas adsorption of CO_2 over CH_4. It exhibited strong fluorescence emission upon excitation at RT, and a selective, efficient emission quenching response towards nitroaromatic explosives.

1 Introduction

Metal–organic frameworks (MOFs) have been extensively researched during the past decade for their intriguing structural diversity and interesting properties such as gas adsorption,[1] photoluminscence,[2] magnetism,[3] and catalysis.[4] Among these, multifunctional MOFs combining luminescence, magnetism, and permanent porosity, *etc.* have been of particular interest because of their potential applications as chemical sensors and devices.[5,6] To tailor MOFs for chemical sensing, one often constructs MOFs with a specific structure and functionality by the deliberate design and selection of organic linkers and metal-containing units, *e.g.* the introduction of guest accessible functional organic sites or open metal sites in MOFs. Appropriately tuned pore sizes and functionalized pore surfaces can initiate differential recognition/binding events with certain guest molecules in MOFs, leading to selective adsorption or molecular sensing.[7]

An alternative approach is to generate charged surfaces or incorporate charged species inside the pores that serve as recognition/binding sites and enhance the host–guest interactions in MOFs.[8,9] Porous anionic frameworks are less common than neutral frameworks because the charge-balancing cations will occupy lots of free space. However, there are some advantages for anionic frameworks as the presence of the cations tunes the pore sizes and the pore surface properties, and thus renders MOFs useful for selective gas separation and highly selective sensing. Herein we report the preparation of a photoluminescent microporous metal organic anionic framework $[In_2L][NH_2(CH_3)_2]_2\cdot(DMF)_4(H_2O)_{16}$ (**1**) (DMF = *N*,*N*′-dimethylformide, L = tetrakis[(3,5-dicarboxyphenoxy)methyl]methane (H_8L), Scheme 1) for selectively sensing nitroaromatic explosives. The origin of such selectivity can be attributed to the selective interactions between the electron-deficient nitroaromatic molecules and the negatively charged pore surface of **1**.

2 Experimental section

2.1 Materials and methods

All reagents and solvents were purchased from commercial sources and used without further purification. Ligand H_8L was prepared as described in ref. 10.

Infrared spectra were obtained on a Bruker Vector 22 spectrophotometer with KBr pellets in the 4000–400 cm^{-1} region. Elemental analyses for C, H, and N were performed on an Elementar Vario MICRO analyzer. Thermogravimetric analysis (TGA) was carried out in a Perkin-Elmer thermal analyzer under nitrogen with a heating rate of 10 °C min^{-1}. Powder X-ray diffraction (PXRD) patterns were collected with a scan speed of

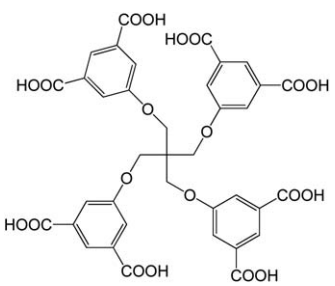

Scheme 1 Schematic structure of H_8L.

[a]State Key Laboratory of Coordination Chemistry, School of Chemistry and Chemical Engineering, Nanjing University, Nanjing, 210093, China. E-mail: hbdu@nju.edu.cn
[b]Department of Chemistry, University of Texas at San Antonio, Texas 78249-0698, USA. E-mail: banglin.chen@utsa.edu
[c]Department of Chemistry, Nanjing University of Technology, Nanjing 210009, China

† Electronic supplementary information (ESI) available: X-ray crystallographic files (CIF), figures of the asymmetric unit, PXRD and TGA. CCDC 909699. For ESI and crystallographic data in CIF see DOI: 10.1039/c3ta01118f

0.1 s per degree on a Bruker D8 Advance instrument using Cu Kα radiation (λ = 1.54056 Å) at room temperature. The gas adsorption isotherms were measured by using a Micromeritics ASAP 2020 volumetric adsorption analyzer. The luminescence spectra were recorded on a Hitachi F-4600 fluorescence spectrophotometer. The glass slides, 10 mm × 30 mm in size, were rinsed with de-ionized water and dried at 60 °C in an oven. Cyanoacrylate adhesive (10 mm × 8 mm) was then applied to the slides. The sample was then sprinkled evenly onto the glued surface of the slide. The sample quantity for each luminescence test was 20 mg. The fluorescence spectra of the glass slide with glue were collected before placing the sample on the glass slide.

2.2 Synthesis

Synthesis of 1. A mixture of $In(NO_3)_3 \cdot 4.5H_2O$ (0.0382 g, 0.1 mmol) and H_8L (0.0158 g, 0.02 mmol) in 6 mL DMF and three drops of HCl (6 mol L^{-1}) was sealed in a Teflon-linear autoclave (25 mL), heated at 160 °C for 1 day, and then slowly cooled down to room temperature. Colorless block single crystals of **1** were collected by filtration, washed with DMF and CH_2Cl_2 and air-dried. Yield 60% (based on H_8L). Elemental analysis for $C_{53}H_{96}N_6In_2O_{40}$, calcd (%): C, 37.85; H, 5.77; N, 4.98. Found (%): C, 37.71; H, 5.74; N, 4.98. FT-IR (KBr, cm^{-1}): 3401 (s), 1663 (s), 1565 (s), 1376 (s), 1257 (s), 1118 (s), 1041 (s), 894 (m), 775 (s), 720 (s), 559 (m), 454 (w).

2.3 Single-crystal X-ray diffraction analysis

Suitable crystals of **1** with the dimensions *ca.* 0.13 × 0.12 × 0.10 mm^3 were selected for single crystal X-ray diffraction. The data were collected at 296 K on a Bruker Smart CCD diffractometer with graphite-monochromatic Kα radiation (λ = 0.71073 Å) from an enhanced optic X-ray tube. Raw data for the structure were obtained using SAINT, and absorption correction was applied using SADABS programs.[11] The structure was solved by the direct method and refined by full-matrix least-squares on F^2, using the SHELXL-97 program.[12] All non-hydrogen atoms were refined anisotropically, and the hydrogen atoms were placed in geometrically calculated positions which were refined using the riding model (except the hydrogens of the guest water and one disorder $NH_2(CH_3)_2^+$ molecule, which were not included in the model). Elemental and TG analyses revealed that the chemical formula of MOF **1** contains sixteen water and four DMF guest molecules. The final formula $[In_2L][NH_2(CH_3)_2]_2 \cdot (DMF)_4(H_2O)_{16}$ was derived from crystallographic data combined with elemental and TGA data. Details of the crystal parameters, data collection and refinement results are summarized in Table 1. Selected bond lengths and angles are shown in Table S1 (ESI†). Further details can be obtained from the ESI.†

Table 1 Crystallographic and structural data for **1**[a]

Compound reference	**1**
Chemical formula	$C_{41}H_{40}In_2N_2O_{22}$
Formula mass	1142.40
Crystal system	Orthorhombic
a/Å	12.262(4)
b/Å	13.572(5)
c/Å	24.934(9)
α/°	90.00
β/°	90.00
γ/°	90.00
Unit cell volume/$Å^3$	4150(2)
Temperature/K	296(2)
Space group	$P222(1)$
No. of formula units per unit cell, Z	2
Absorption coefficient, μ/mm^{-1}	0.603
No. of reflections measured	27 989
No. of independent reflections	7643
R_{int}	0.0660
Final R_1 values ($I > 2\sigma(I)$)	0.0992
Final w$R(F^2)$ values ($I > 2\sigma(I)$)	0.2645
Final R_1 values (all data)	0.1404
Final w$R(F^2)$ values (all data)	0.2949
Goodness of fit on F^2	1.034

[a] $R_1 = \Sigma||F_o| - |F_c||/\Sigma|F_o|$, $wR = [\Sigma w(F_o^2 - F_c^2)^2/\Sigma w(F_o^2)^2]^{1/2}$.

3 Results and discussion

3.1 Synthesis

H_8L is a flexible organic linker with a combination of *m*-benzenedicarboxylate moieties and a tetrahedral geometry, and has been used to construct robust MOFs with a rare (4,8)-connected *scu* topology for gas storage.[10,13] In this study, indium ions were used as the metal connectors in the construction of **1** because the flexible coordination number of In^{3+} (*e.g.* from 6 to 8) often leads to MOFs with intriguing structures and properties.[9,14] Particularly, the uneven charges on In make it an ideal candidate to prepare anionic frameworks.[9]

MOF **1** was solvothermally synthesized from the self-assembly of $In(NO_3)_3 \cdot 4.5H_2O$ and H_8L in DMF. The phase purity was confirmed by elemental analyses and PXRD. Crystals of MOF **1** are stable in common organic solvents such as ethanol, DMF, chloroform, benzene, and nitrobenzene.

3.2 Crystal structure descriptions

Single-crystal X-ray diffraction analysis revealed that MOF **1** crystallizes in the $P222(1)$ space group with two asymmetric units in the unit cell. The asymmetric unit contains two crystallographically independent In(III) ions, a half L^{8-} ligand, and three $(CH_3)_2NH_2^+$ counterions (Fig. S1 in ESI†). As shown in Fig. 1, the In(1) ion is six-coordinated by four oxygen atoms from two chelating carboxyl groups and two oxygen atoms from two monodentate carboxyl groups, giving rise to a distorted octahedral geometry. The In(2) ion is eight-coordinated by eight oxygen atoms from four chelating carboxyl groups to form a dodecahedral motif. The In–O distances and O–In–O bond angles range from 2.112(6) to 2.434(7) Å and 53.9(2) to 174.9(3)°, respectively, which are comparable with those observed in other In(III)–carboxylate frameworks.[14] Both In atoms are four-connected, coordinating to four L ligands. The L ligand, on the other hand, is fully deprotonated, coordinating to eight indium centers in a cuboid geometry *via* chelating bis- and mono-dentate carboxylate groups.

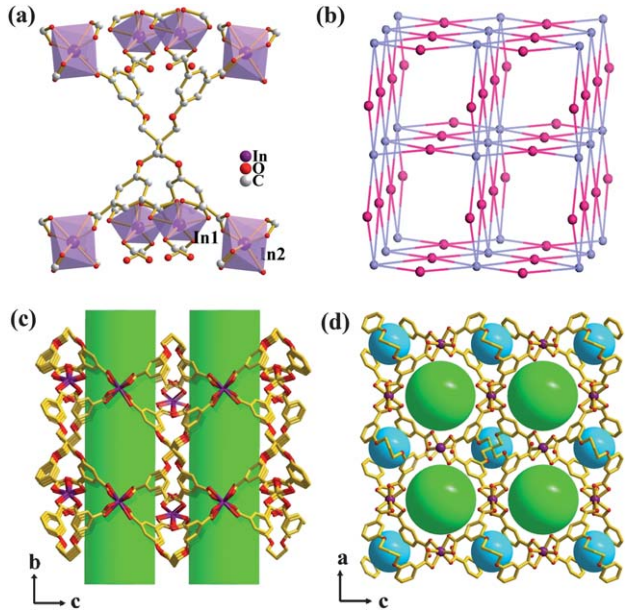

Fig. 1 Views of (a) the organic ligand which is connected to eight In atoms, (b) the resulting 4,8-connected framework with *scu* topology, and structures viewed along (c) the *a* axis and (d) the *b* axis to illustrate the pore windows and corresponding interconnecting cages A (blue) and B (green) in **1**.

The structure of **1** is constructed from 4-connected In centers and 8-connected L ligands, which form an anionic open framework with interconnecting channels of approximately 7.0 × 5.5, 6.2 × 6.2, and 6.2 × 6.2 Å^2 (taking account of the van der Waals radii) along the *a*-, *b*- and *c*-axes, respectively (Fig. 1). Inside these channels are located charge-balancing $NH_2(CH_3)_2^+$ counterions and DMF and H_2O guest molecules. The $(CH_3)_2NH_2^+$ cations were likely generated *via* the decomposition of DMF under solvothermal conditions, which is not without precedent.[15] The intersecting of the channels yields two types of cages in **1**: cage A is an octahedral cage composed of four In(III) ions and four isophthalate units from two ligands, and cage B is a slightly distorted cuboctahedral cage composed by eight In(III) ions and four isophthalate units (Fig. 1d). The approximate diameters of the inner spheres of cages A and B are 4.2 Å and 8.8 Å, respectively. Each cage A is linked to eight B cages *via* sharing triangular faces and *vice versa*, to form an open framework of **1**. From the topological viewpoint, **1** can be considered as a rare (4,8)-connected *scu* net with the point symbol of $\{4^4 6^2\}_2\{4^{16}6^{12}\}$. Therefore, **1** is one of the few known MOFs with *scu* topology.[10,13,16] MOF **1** possesses a highly open framework. The guest accessible volume (1822.7 Å^3 per unit cell) comprises 43.9% of the crystal volume, as calculated by the PLATON program.[17]

3.3 Thermal properties

To investigate the thermal stability of the framework of **1**, TG analysis was carried out. As shown in Fig. S2 (ESI†), MOF **1** began to lose its solvent molecules from *ca.* 50 to *ca.* 260 °C, with further significant weight loss up to 500 °C attributable to the departure of charge-balancing $(CH_3)_2NH_2^+$ cations and the decomposition of the ligands. TGA study indicated that the filled solvent molecules could be partially removed while the framework remained intact. The robustness and thermal stabilities of the framework of **1** were further checked by X-ray powder diffraction. Fig. S3 (ESI†) shows that the main XRD peaks of **1** heated at 80 °C under vacuum for 12 h basically matched those of the pristine one, indicating that the framework of **1** remained intact after desolvation and activation.

3.4 Adsorption properties

The permanent porosity of MOF **1** was confirmed by gas adsorption measurements. Before the measurements, the samples of **1** were activated by evacuation at 80 °C under dynamic vacuum overnight. As shown in Fig. 2, N_2 adsorption and desorption isotherms at 77 K are typical of type-I behavior, characteristic of microporous materials. The Brunauer–Emmett–Teller (BET) and the Langmuir surface areas were calculated as 752 and 991 m^2 g^{-1}, respectively. The Horvath–Kawazoe (HK) model[18] indicates a median pore diameter of 6.1 Å in MOF **1**, which is consistent with those calculated from the single crystal structure analysis when taking account of the van der Waals radii.

As shown in Fig. 3, activated **1** takes up 125 cm^3 g^{-1} (1.12 wt%) of H_2 at 77 K and 760 Torr. Because the H_2 sorption isotherm of MOF **1** is not fully saturated, a higher hydrogen sorption capacity may be expected under higher pressures. It is also noted that MOF **1** takes up much higher amounts of carbon dioxide (61.7 cm^3 g^{-1} or 2.75 mmol g^{-1} at 273 K and 1 atm, 29.7 cm^3 g^{-1} or 1.32 mmol g^{-1} at 293 K at 1 atm) than methane (4.0 cm^3 g^{-1} or 0.177 mmol g^{-1} at 273 K and 1 atm, and 3.8 cm^3 g^{-1} or 0.168 mmol g^{-1} at 293 K and 1 atm) under the same conditions (Fig. 3). The adsorbed CO_2/CH_4 molar ratios are 15.5 at 273 K and 7.8 at 293 K, respectively, highlighting MOF **1** as a potential material for the selective separation of CO_2/CH_4.[19,20] The selective adsorption of CO_2 over CH_4 may be the result of the combination of the kinetic diameter and quadrupole moment differences between the two gas molecules.[21]

3.5 Photoluminescent properties

MOF **1** exhibited a strong fluorescent emission peak at 360 nm upon excitation at 280 nm at RT (Fig. S4 in ESI†), which is

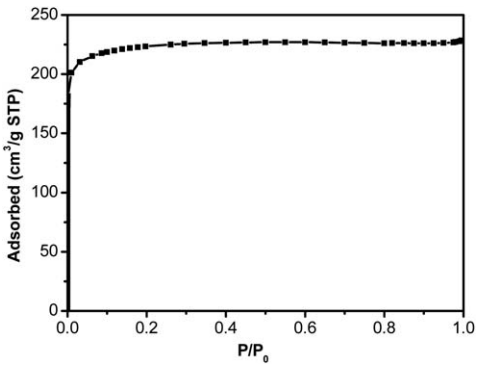

Fig. 2 Gas adsorption isotherms of **1** for N_2 at 77 K.

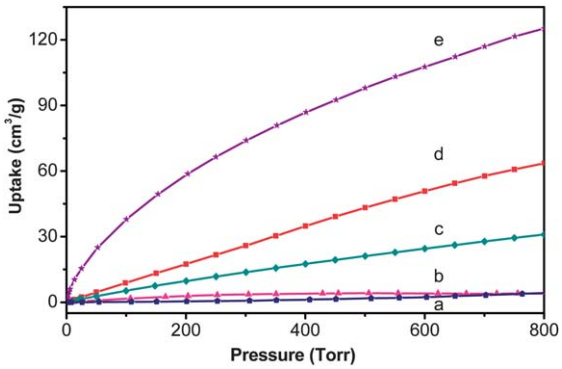

Fig. 3 Gas adsorption isotherms of **1** for (a) CH_4 at 293 K, (b) CH_4 and 273 K, (c) CO_2 at 293 K, (d) CO_2 at 273 K, and (e) H_2 at 77 K.

blue-shifted in comparison with the free ligand (420 nm). This emission band can be attributed to the $\pi^* \rightarrow \pi$ transition involving a ligand-centered excited state.[22] The fluorescent emission of MOF **1** showed very small solvent-dependence, the emission maximum being slightly blue-shifted when the samples were immersed into DMF (349 nm) and EtOH (348 nm). It is interesting to note that the emission intensities of MOF **1** varied upon contact with different solvents (Fig. 4). While there were slight changes in the intensities in common solvents such as MeOH and EtOH compared to that in DMF, aromatics with electron-donating groups significantly enhanced the luminescence emission of **1**. Toluene enhanced the emission intensity by 175% compared to that in DMF, followed by *p*-xylene (170%) and chlorobenzene (110%). On the other hand, nitroaromatics such as nitrobenzene (NB), 1,3-DNB (1,3-dinitrobenzene) and 2,4-DNT (2,4-dinitrotoluene) significantly quenched the emission. In comparison, the aliphatic 1-nitropropane showed inefficient quenching (16% reduction in intensity), while the inorganic nitrate enhanced the photoluminescence. These results are similar to those reported by Li *et al.*,[6a,b] demonstrating **1** is one of the few known MOFs useful for the detection of high explosives.[6]

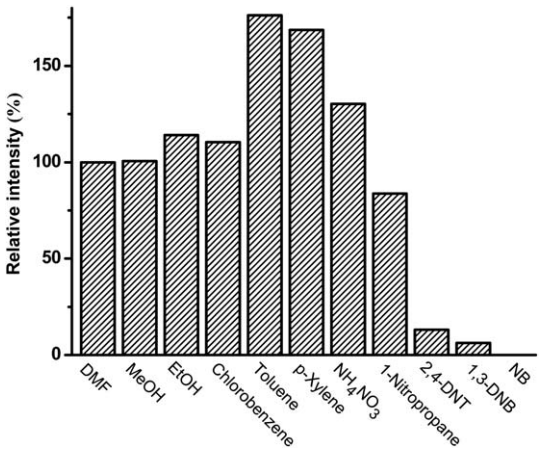

Fig. 4 Percentage of fluorescence quenching or enhancement after the samples were immersed into different analytes (0.5 mol L^{-1}) in DMF for 2 min at room temperature (excited at 280 nm).

To explore the sensing capability for nitroaromatic explosives, the emission spectra of tape-glued crystals of MOF **1** were recorded upon immersion in DMF solutions of NB, 1,3-DNB or 2,4-DNT. Fig. 5 shows the relationships between the luminescence quenching of **1** and the concentrations of NB, 1,3-DNB or 2,4-DNT. The most effective quencher is NB and the least effective is 2,4-DNT. The maximum fluorescence intensity of **1** was reduced by 81.5%, 46.2% and 14.0% upon exposure to 5×10^{-6} mol L^{-1} of NB, 1,3-DNB and 2,4-DNT, respectively, highlighting that **1** is amongst the most efficient porous material-based sensors for nitroaromatic explosives.[6]

The excellent fluorescence quenching response to nitroaromatics can be attributed to the electrostatic interactions between the anionic framework of **1** and the electron-deficient

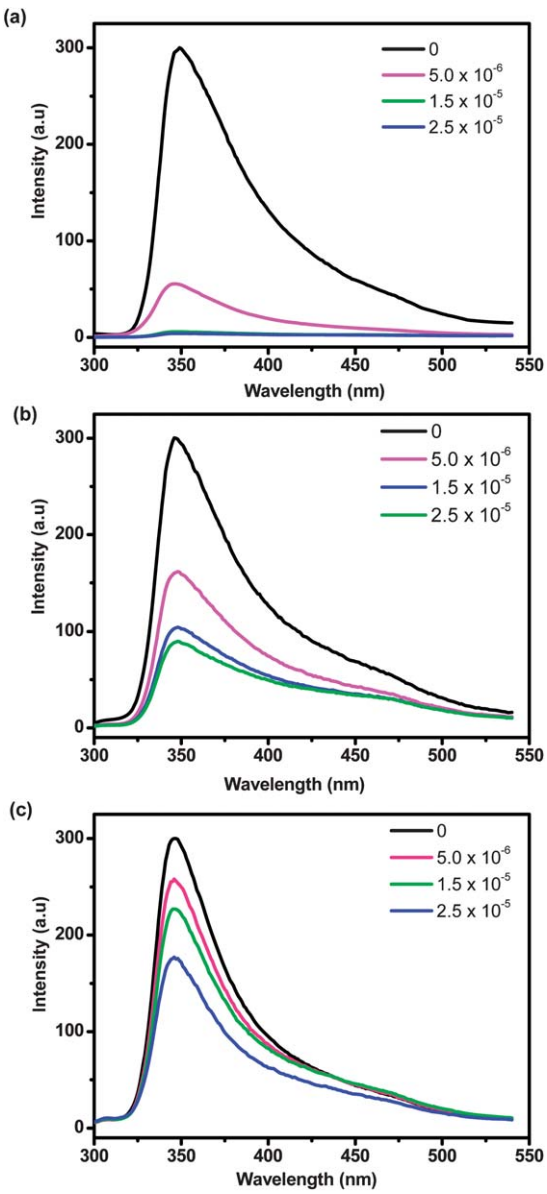

Fig. 5 Quenching response of **1** before and after exposure to different concentrations (mol L^{-1}) of (a) NB, (b) 1,3-DNB, and (c) 2,4-DNT in DMF solution for 2 min (excited at 280 nm).

nitroaromatic analytes. The more electron-withdrawing groups there are on an analyte, the more efficient the fluorescence quenching response (*i.e.* 1,3-DNB > 2,4-DNT). However, the fluorescence quenching response is also related to the pore confinement of the analyte inside the cavities of **1**. The sizes of the pores in **1** calculated from the X-ray crystal structure analysis are *ca.* 7.0 × 5.5, 6.2 × 6.2, 6.2 × 6.2 Å along the *a*-, *b*- and *c*-axes, respectively. These would allow NB (kinetic diameter *ca.* 5.9 Å (ref. 23)) to pass through, but make it hard for 1,3-DNB or 2,4-DNT molecules (kinetic diameters >7.0 Å considering that the kinetic diameters of *meta*- and *ortho*-xylene are 7.1 and 7.4 Å, respectively[24]) to enter. This explains the fact that **1** is more sensitive towards NB than 1,3-DNB or 2,4-DNT.

The diffusion-controlled fluorescence quenching response of **1** to nitroaromatics was further confirmed by vapor-sensing experiments. As shown in Fig. 6, the fluorescence emission of **1** was quenched by 82% within 5 s when exposed to saturated NB vapor (*ca.* 400 ppm (ref. 25)) at RT. The quench percentages appeared to approach a constant level given enough exposure time. In comparison, the quench responses to saturated vapors of 1,3-DNB and 2,4-DNT were much slower. Although the lower vapor pressures of 1,3-DNB (*ca.* 5.7 ppm (ref. 26)) and 2,4-DNT (*ca.* 0.2 ppm (ref. 25)) contribute to their slower responses, these may also be attributed to the fact that in the latter cases the quench occurred mainly at the external surfaces of the MOF **1** crystals. As mentioned earlier, the pores of MOF **1** are too small for 1,3-DNB or 2,4-DNT molecules and it may take a relatively long time for these molecules to diffuse into the pores. These results suggest that reducing the size of the crystals of **1** should result in faster responses.

4 Conclusions

We have successfully synthesized the novel microporous coordination polymer $[In_2L][NH_2(CH_3)_2]_2\cdot(DMF)_4(H_2O)_{16}$ with a (4,8)-connected *scu* net and highly selective gas adsorption of CO_2 over CH_4. It possesses a photoluminescent anionic open framework, and exhibits highly selective and efficient emission quenching response upon interaction with nitroaromatic explosives, making it a promising sensory material for explosives monitoring. This work shows that the charged framework surface can interact with guest molecules, leading to selective adsorption or molecular sensing, and thus provide an alternative route to prepare functional MOFs.

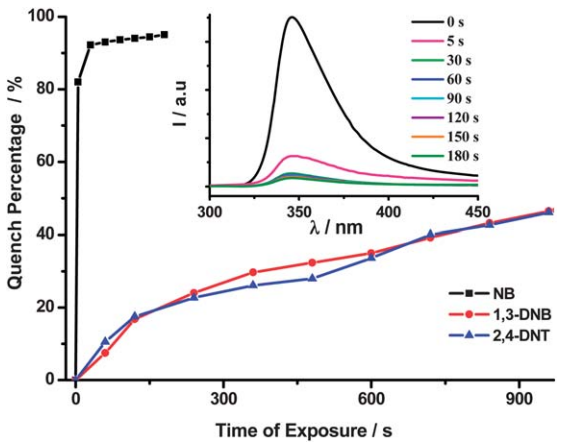

Fig. 6 Fluorescence quench response of **1** upon exposure to saturated vapours of NB, 1,3-DNB, and 2,4-DNT at room temperature for the specified times. Inset: the corresponding fluorescent spectra of **1** upon exposure to NB vapour at the specified exposure times (excited at 280 nm).

Acknowledgements

We are grateful for financial support from the National Basic Research Program (2011CB808704), the National Natural Science Foundation of China (21021062 and 20931004), and the Fundamental Research Funds for the Central Universities (1114020502).

Notes and references

1 (*a*) J. R. Li, R. J. Kuppler and H. C. Zhou, *Chem. Soc. Rev.*, 2009, **38**, 1477; (*b*) B. L. Chen, S. C. Xiang and G. D. Qian, *Acc. Chem. Res.*, 2010, **43**, 1115.
2 (*a*) Y. Cui, Y. Yue, G. Qian and B. Chen, *Chem. Rev.*, 2012, **112**, 1126; (*b*) M. D. Allendorf, C. A. Bauer, R. K. Bhakta and R. J. T. Houk, *Chem. Soc. Rev.*, 2009, **38**, 1330.
3 M. Kurmoo, *Chem. Soc. Rev.*, 2009, **38**, 1353.
4 (*a*) A. U. Czaja, N. Trukhan and U. Muller, *Chem. Soc. Rev.*, 2009, **38**, 1284; (*b*) A. Corma, H. García and F. X. Llabres i Xamena, *Chem. Rev.*, 2010, **110**, 4606.
5 L. E. Kreno, K. Leong, O. K. Farha, M. Allendorf, R. P. Van Duyne and J. T. Hupp, *Chem. Rev.*, 2012, **112**, 1105.
6 (*a*) A. Lan, K. Li, H. Wu, D. H. Olson, T. J. Emge, W. Ki, M. Hong and J. Li, *Angew. Chem., Int. Ed*, 2009, **48**, 2334; (*b*) S. Pramanik, C. Zheng, X. Zhang, T. J. Emge and J. Li, *J. Am. Chem. Soc.*, 2011, **133**, 4153; (*c*) C. Zhang, Y. Che, Z. Zhang, X. Yang and L. Zang, *Chem. Commun.*, 2011, **47**, 2336; (*d*) H. Xu, F. Liu, Y. Cui, B. Chen and G. Qian, *Chem. Commun.*, 2011, **47**, 3153.
7 L. J. Murray, M. Dinca and J. R. Long, *Chem. Soc. Rev.*, 2009, **38**, 1294.
8 (*a*) Z. Wang and S. M. Cohen, *Chem. Soc. Rev.*, 2009, **38**, 1315; (*b*) D. Sun, Y. Ke, D. J. Collins, G. A. Lorigan and H.-C. Zhou, *Inorg. Chem.*, 2007, **46**, 2725; (*c*) Q.-G. Zhai, Q. Lin, T. Wu, L. Wang, S.-T. Zheng, X. Bu and P. Feng, *Chem. Mater.*, 2012, **24**, 2624.
9 (*a*) S. Yang, X. Lin, A. J. Blake, G. S. Walker, P. Hubberstey, N. R. Champness and M. Schröder, *Nat. Chem.*, 2012, **1**, 487; (*b*) Q.-G. Zhai, Q. Lin, T. Wu, L. Wang, S.-T. Zheng, X. Bu and P. Feng, *Chem. Mater.*, 2012, **24**, 2624; (*c*) L. Wang, T. Song, L. Huang, J. Xu, C. Li, C. Ji, L. Shan and L. Wang, *CrystEngComm*, 2011, **13**, 4005; (*d*) J.-M. Gu, S.-J. Kim, Y. Kim and S. Huh, *CrystEngComm*, 2012, **14**, 1819; (*e*) S. Yang, G. S. B. Martin, J. J. Titman, A. J. Blake, D. R. Allan, N. R. Champness and M. Schröder, *Inorg. Chem.*, 2011, **50**, 9374; (*f*) T. Lee, Z. X. Liu and H. L. Lee, *Cryst. Growth Des.*, 2011, **11**, 4146; (*g*) K. C. Stylianou, R. Heck, S. Y. Chong, J. Bacsa, J. T. A. Jones,

Y. Z. Khimyak, D. Bradshaw and M. J. Rosseinsky, *J. Am. Chem. Soc.*, 2010, **132**, 4119.
10 Y. S. Xue, Y. B. He, S. B. Ren, Y. F. Yue, L. Zhou, Y. Z. Li, H. B. Du, X. Z. You and B. L. Chen, *J. Mater. Chem.*, 2012, **22**, 10195.
11 *SMART and SADABS*, Bruker AXS Inc., Madison, Wisconsin, USA, 2002.
12 G. M. Sheldrick, *Acta Crystallogr., Sect. A: Found. Crystallogr.*, 2008, **64**, 112.
13 (*a*) Z. J. Lin, T. F. Liu, B. Xu, L. W. Han, Y. B. Huang and R. Cao, *CrystEngComm*, 2011, **13**, 3321; (*b*) Z. J. Lin, T. F. Liu, X. L. Zhao, J. Lv and R. Cao, *Cryst. Growth Des.*, 2011, **11**, 4284; (*c*) W. J. Zhuang, D. Q. Yuan, D. H. Liu, C. L. Zhong, J. R. Li and H. C. Zhou, *Chem. Mater.*, 2012, **24**, 18; (*d*) Y. Q. Lan, H. L. Jiang, S. L. Li and Q. Xu, *Inorg. Chem.*, 2012, **51**, 7484.
14 (*a*) Z. Z. Lin, F. L. Jiang, D. Q. Yuan, L. Chen, Y. F. Zhou and M. C. Hong, *Eur. J. Inorg. Chem.*, 2005, 1927; (*b*) Z. Z. Lin, F. L. Jiang, L. Chen, C. Y. Yue, D. Q. Yuan, A. J. Lan and M. C. Hong, *Cryst. Growth Des.*, 2007, **7**, 1712; (*c*) B. Gomez-Lor, E. Gutiérrez-Puebla, M. Iglesias, M. A. Monge, C. Ruiz-Valero and N. Snejko, *Inorg. Chem.*, 2002, **41**, 2429; (*d*) J. Zhang, S. M. Chen, T. Wu, P. Y. Feng and X. H. Bu, *J. Am. Chem. Soc.*, 2008, **130**, 12882; (*e*) S. M. Chen, J. Zhang, T. Wu, P. Y. Feng and X. H. Bu, *J. Am. Chem. Soc.*, 2009, **131**, 16027.
15 A. D. Burrows, K. Cassar, T. Duren, R. M. W. Friend, M. F. Mahon, S. P. Rigby and T. L. Savaresea, *Dalton Trans.*, 2008, 2465.
16 (*a*) C. R. Tan, S. H. Yang, N. R. Champness, X. Lin, A. J. Blake, W. Lewis and M. Schröder, *Chem. Commun.*, 2011, **47**, 4487; (*b*) Y.-S. Xue, F.-Y. Jin, L. Zhou, M.-P. Liu, Y. Xu, H.-B. Du, M. Fang and X.-Z. You, *Cryst. Growth Des.*, 2012, **12**, 6158.
17 A. L. Spek, *J. Appl. Crystallogr.*, 2003, **36**, 7.
18 G. Horvath and K. Kawazoe, *J. Chem. Eng. Jpn.*, 1983, **16**, 470.
19 (*a*) Z. J. Zhang, S. C. Xiang, X. T. Rao, Q. Zheng, F. R. Fronczek, G. D. Qian and B. L. Chen, *Chem. Commun.*, 2010, **46**, 7205; (*b*) Z. J. Zhang, S. C. Xiang, Y. S. Chen, S. Q. Ma, Y. Lee, T. P. Bobin and B. L. Chen, *Inorg. Chem.*, 2010, **49**, 8444; (*c*) Z. X. Chen, S. C. Xiang, H. D. Arman, J. U. Mondal, P. Li, D. Y. Zhao and B. L. Chen, *Inorg. Chem.*, 2011, **50**, 3442; (*d*) G. Ortiz, S. Brand, Y. Rousselin and R. Guilard, *Chem.–Eur. J.*, 2011, **17**, 6689; (*e*) Y. X. Hu, S. C. Xiang, W. W. Zhang, Z. X. Zhang, L. Wang, J. F. Bai and B. L. Chen, *Chem. Commun.*, 2009, 7551; (*f*) L. Hou, W. J. Shi, Y. Y. Wang, Y. Guo, C. Jin and Q. Z. Shi, *Chem. Commun.*, 2011, **47**, 5464; (*g*) S. Henke and R. A. Fischer, *J. Am. Chem. Soc.*, 2011, **133**, 2064.
20 (*a*) B. S. Zheng, J. F. Bai, J. G. Duan, L. Wojtas and M. J. Zaworotko, *J. Am. Chem. Soc.*, 2011, **133**, 748; (*b*) S. M. Zhang, Z. Chang, T. L. Hu and X. H. Bu, *Inorg. Chem.*, 2010, **49**, 11581; (*c*) Y. G. Lee, H. R. Moon, Y. E. Cheon and M. P. Suh, *Angew. Chem., Int. Ed*, 2008, **47**, 7741.
21 (*a*) Y.-S. Bae, K. L. Mulfort, H. Frost, P. Ryan, S. Punnathanam, L. J. Broadbelt, J. T. Hupp and R. Q. Snurr, *Langmuir*, 2008, **24**, 8592; (*b*) Y. E. Cheon and M. P. Suh, *Chem. Commun.*, 2009, 2296; (*c*) A. J. Lan, K. H. Li, H. H. Wu, L. Z. Kong, N. Nijem, D. H. Olson, T. J. Emge, Y. J. Chabal, D. C. Langreth, M. C. Hong and J. Li, *Inorg. Chem.*, 2009, **48**, 7165.
22 (*a*) J. R. Lakowicz, *Principles of Fluorescence Spectroscopy*, Springer, Berlin, 3rd edn, 2006; (*b*) B. Valeur. *Molecular Fluorescence: Principles and Application*, Wiley-VCH, Weinheim, 2002.
23 J. Reungoat, J. S. Pic, M. H. Manéro and H. Debellefontaine, *Sep. Sci. Technol.*, 2007, **42**, 1447.
24 A. Corma, F. Llopis and J. B. Monton, in *New Frontiers in Catalysis*, ed. L. Guczi, F. Solymosi and P. Tétényi, Elsevier, Amsterdam, *Stud. Surf. Sci. Catal.*, 1993, vol. 75, p. 1145.
25 Q. Fang, J. Geng, B. Liu, D. Gao, F. Li, Z. Wang, G. Guan and Z. Zhang, *Chem.–Eur. J.*, 2009, **15**, 11507.
26 R. Orghici, P. Lützow, J. Burgmeier, J. Koch, H. Heidrich, W. Schade, N. Welschoff and S. Waldvogel, *Sensors*, 2010, **10**, 6788.

